Supplementary Information

# Controlled synthesis of ternary acrylamide/sodium acrylate/polyethyleneglycol hybrids by integrating different clays and fillers: A comprehensive evaluation of structural features

**Rabia BOZBAY[a,b], Mertcan ER[a,b], Kübra KARA ERSOY[b] and Nermin ORAKDOGEN[a,*]**

[a]Istanbul Technical University, Faculty of Science and Letters, Department of Chemistry, Soft Materials Research Laboratory, 34469, Maslak, Istanbul, Turkey, Tel: +90-212-285-3305.

[b]Graduate School of Science Engineering and Technology, Department of Chemistry, Istanbul Technical University, 34469, Istanbul, Turkey
*Corresponding author; e-mail: orakdogen@itu.edu.tr

## Structural characterization of hybrid PAN/PEG-NC gels-doped with different fillers

**Table S1.** Chemical composition and basic properties of clay minerals used in this work.

| Clay | Chemical Formula | CEC (mmol/ 100 g) | Surface Area ($m^2/g$) | Layer Structure | Average particle size | Family of Clay |
|---|---|---|---|---|---|---|
| **Kaolin** | $Al_2Si_2O_5(OH)_4.nH_2O$ | 3-15 | 10-20 [14] | 1:1 | Hexagonal crystals ranging in size from 0.1 to 30 µm. These crystals form in stacked layers | Kaolinite-serpentine |
| **Bentonite** | $(Na)_{0.7}(Al_{3.3}Mg_{0.7})Si_8O_{20}(OH)_4.nH_2O$ | For Ca-bentonite; 50 and for Na-bentonite; 80-85 | 60-120 for Ca-bentonite and 20-30 for Na-bentonite [15] | 2:1 | 2.5 to 45 µm with a silky-smooth powder | Dioctahedral Smectite |
| **Mica** | $KAl_2[AlSi_3O_{10}](OH)_2$ | 10-70 | 100 [16] | 2:1 | Diameters of crystalline grains are less than 10 µm with an average value of 5.4 µm. Average thickness of grains is 0.8 µm with ratio of diameter to thickness of 6.9 | 2:1 phyllosilicates |

**Table S2.** Constituents of blank PAN/PEG and ternary hybrid PAN/PEG-NC gels.

| Nanofiller content of hybrid gels C = % (w/v) in reaction solution | 1.50 w/v% |
|---|---|
| AAm content | 94 mol% |
| Ionic comonomer NaA content | 6 mol% |
| PEG-2000 content of ternary hybrid gels | 5.14 w/v% |
| Crosslinker ratio *X* (mole ratio of BAAm to monomers AAm + NaA) | 1/82 |
| APS conc | 2.63 mM |
| TEMED conc. | 24.9 mM (0.375 v/v%) |
| Polymerization solvent | Water |
| Type of nanoparticles | Bentonite, kaolin, mica, silica, graphene |

**Table S3.** Data showing % mass loss of clays and nanofillers at temperatures 120 $^{o}$C and 800 $^{o}$C.

| Sample | Weight loss % at 120 $^{o}$C | Weight loss % at 800 $^{o}$C |
|---|---|---|
| Kaolin | 99.4 | 88.3 |
| Bentonite | 86.3 | 80.5 |
| Silica | 93.3 | 90.1 |
| Mica | 99.9 | 99.1 |
| Graphene | 91.4 | 79.3 |

**Table S4.** Thermodegradation data of blank PAN/PEG and filler-doped hybrid PAN/PEG-NC gels. Tmax is the temperature of maximum degradation rate in each stage, ML is the mass loss percentage during the degradation stage and Mr is the residue weight at 650 $^{o}$C.

| Sample code | $Tmax_1$ ( $^{o}$C) | $ML_1$ (%) | $Tmax_2$ ( $^{o}$C) | $ML_2$ (%) | $Tmax_3$ ( $^{o}$C) | $ML_3$ (%) | Mr (%) |
|---|---|---|---|---|---|---|---|
| Blank PAN/PEG | 195.5 | 88.2 | 249.9 | 80.5 | 347.4 | 58.3 | 19.5 |
| PAN/PEG-NC/Kln | 193.9 | 89.9 | 260.9 | 81.8 | 347.5 | 66.3 | 32.6 |
| PAN/PEG-NC/Bnt | 191.2 | 88.8 | 253.7 | 81.5 | 347.9 | 59.5 | 21.4 |
| PAN/PEG-NC/Slc | 189.3 | 88.9 | 253.0 | 79.4 | 347.5 | 58.1 | 18.8 |
| PAN/PEG-NC/Mica | 192.2 | 91.2 | 252.1 | 83.5 | 349.1 | 60.9 | 27.9 |
| PAN/PEG-NC/Grn | - | - | 250.0 | 85.6 | 345.4 | 72.3 | 42.4 |

**Elasticity of hybrid PAN/PEG-NC gels-doped with different fillers**

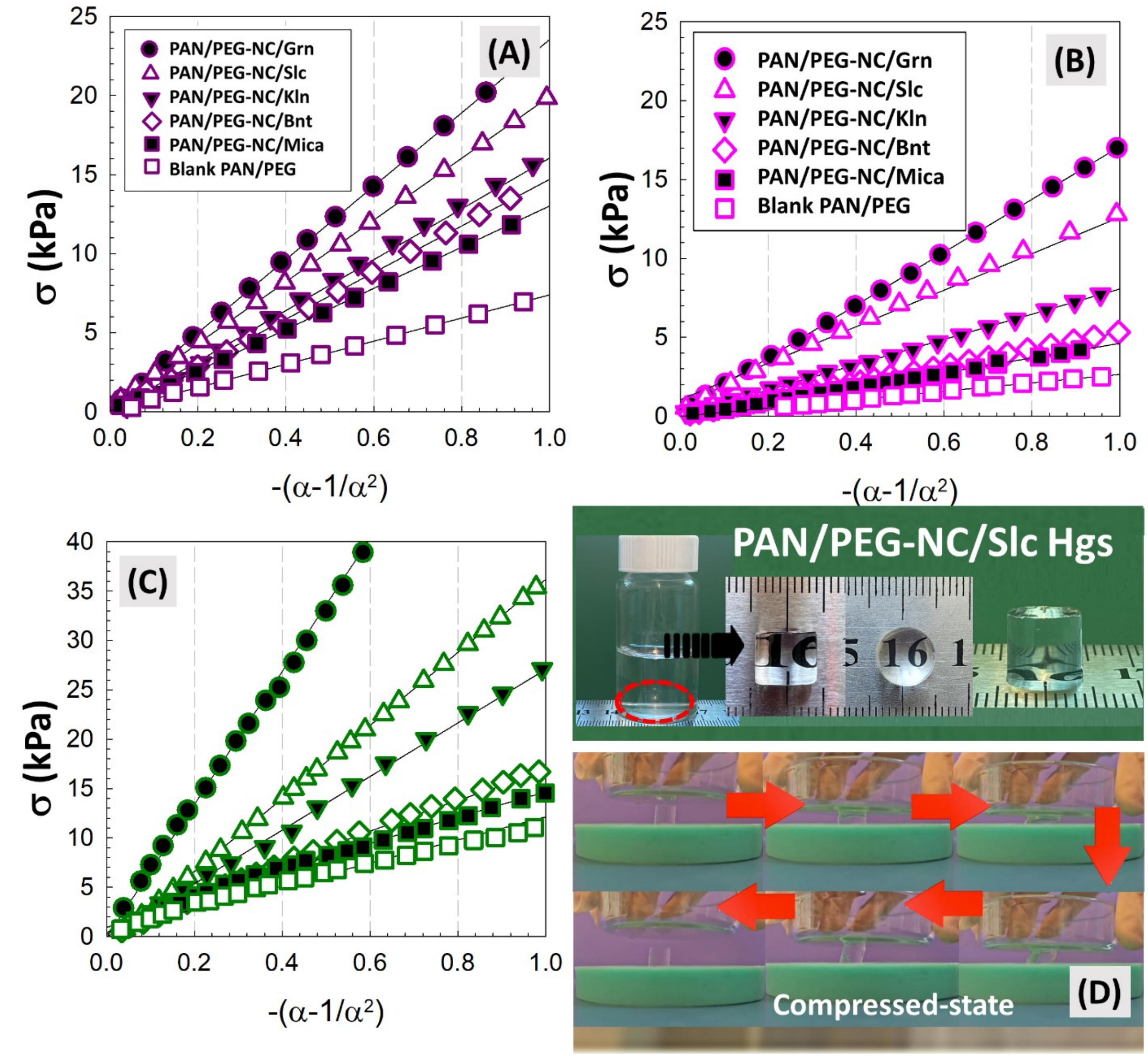


**Fig. S1.** Stress-strain isotherms of hybrid PAN/PEG-NC Hgs (A, B) and Cgs (C) as-prepared state and at thermodynamic equilibrium swollen state. (D) Optical images of Slc-integrated PAN/PEG-NC/Slc hydrogels during uniaxial compression.

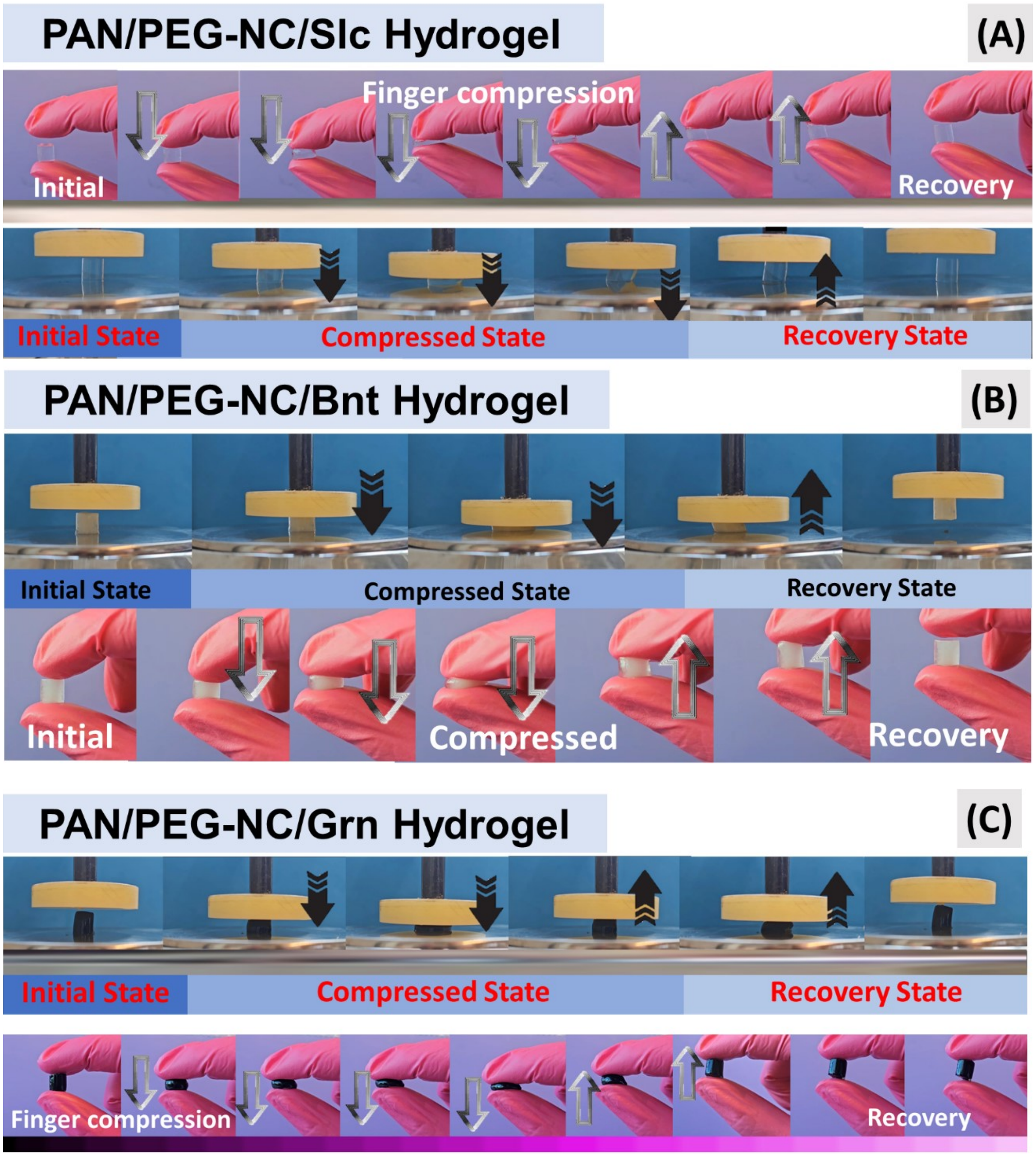


**Figure S2.** Behavior of Slc-integrated PAN/PEG-NC/Slc (A), BNT-integrated PAN/PEG-NC/Bnt (B) and Grn-integrated PAN/PEG-NC/Grn (C) sample during the uniaxial compression and finger testing; before and after removal of stress.

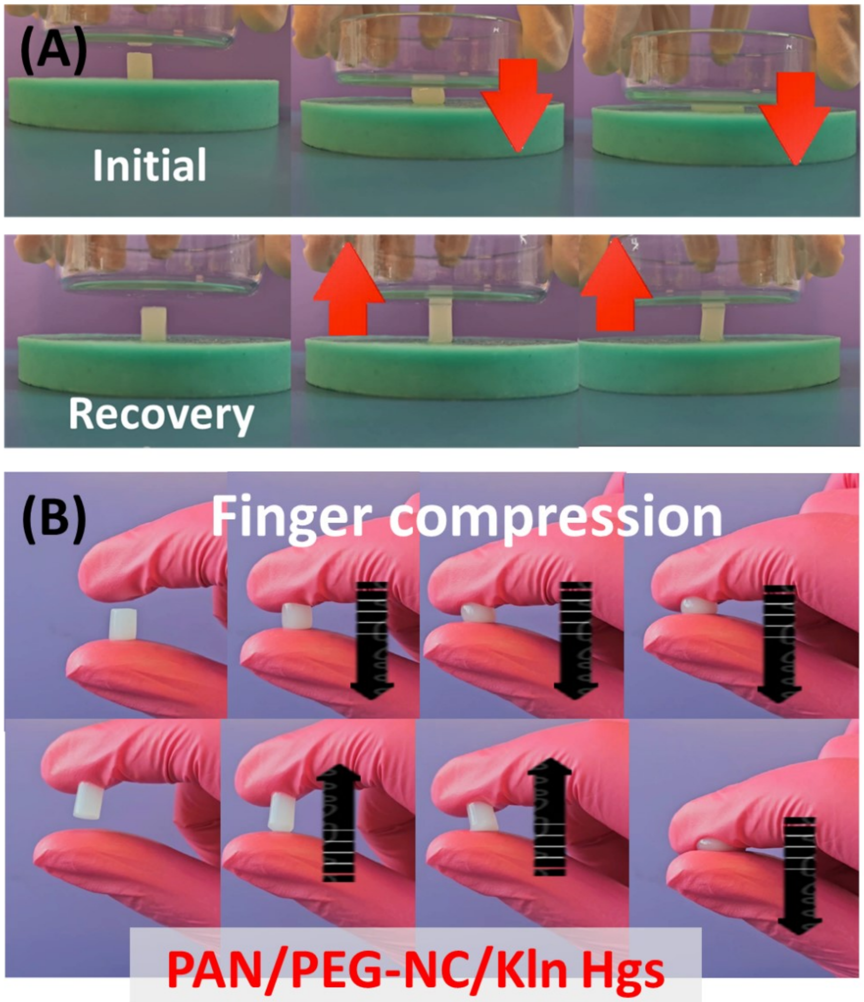


**Figure S3.** Optical appearances of manuel compression with a plate (A) and finger compression (B) of KLN-integrated hybrid PAN/PEG-NC/Kln hydrogels.

**Swelling of hybrid PAN/PEG-NC gels-doped with different fillers**

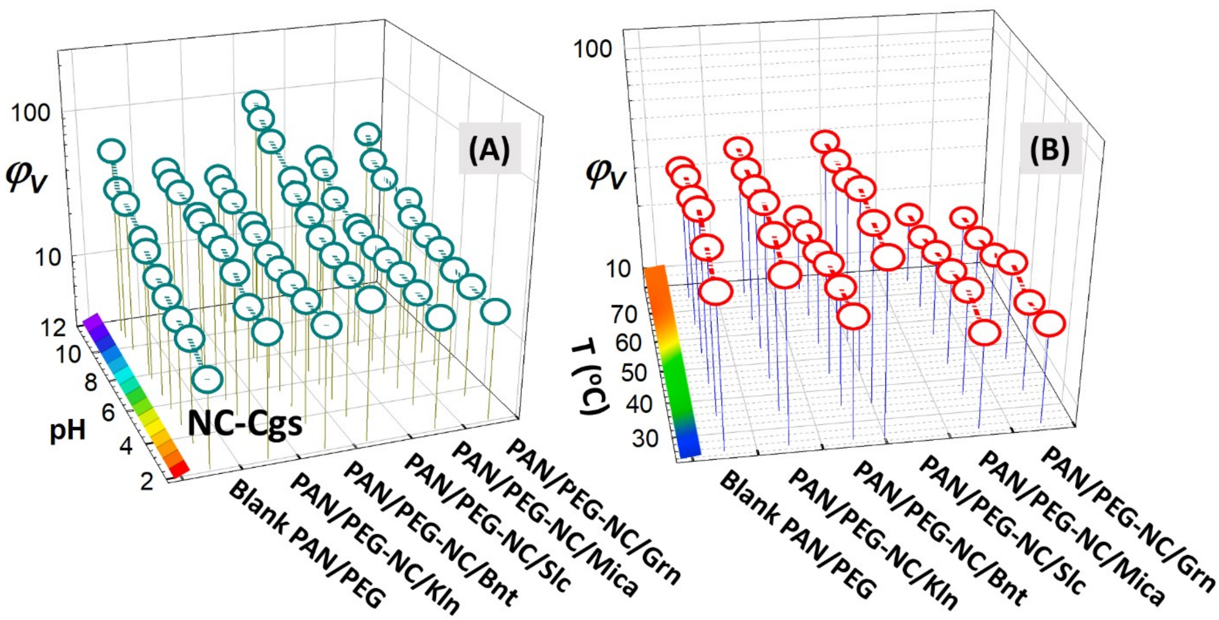


**Figure S4.** The equilibrium volume swelling ratio $\varphi_V$ of hybrid PAN/PEG-NC cryogels as a function of swelling pH(A), and swelling temperature (B).

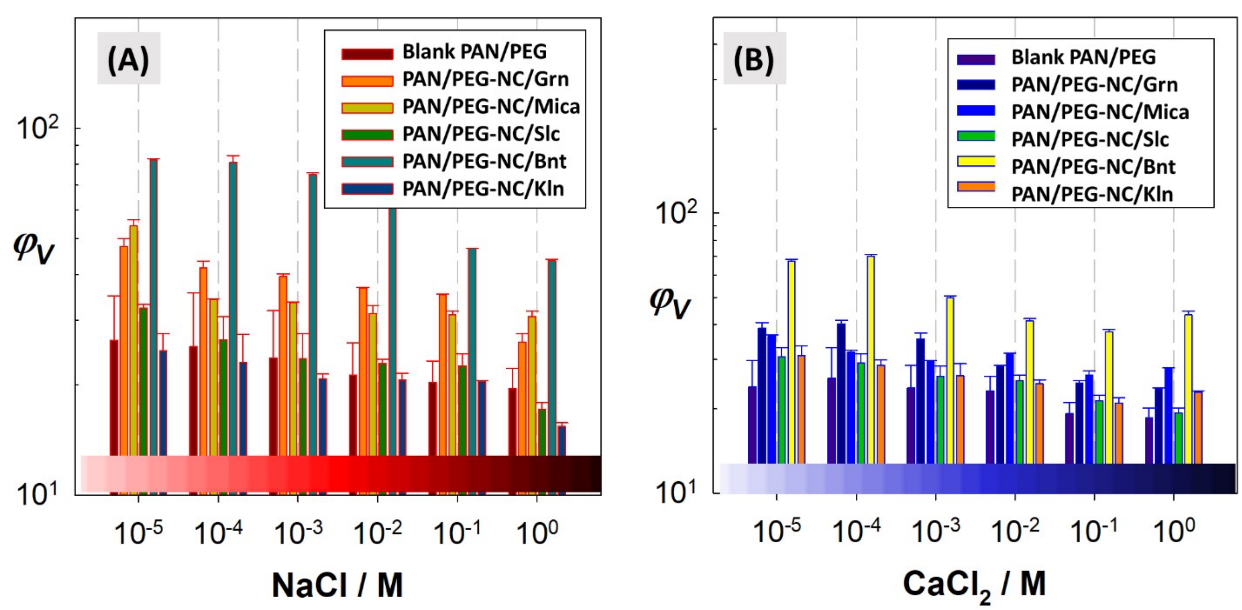


**Figure S5.** The equilibrium volume swelling ratio $\varphi_V$ of hybrid PAN/PEG-NC cryogels as a function of the ionic strength of salt solution of NaCl (A) and $CaCl_2$ (B), respectively.

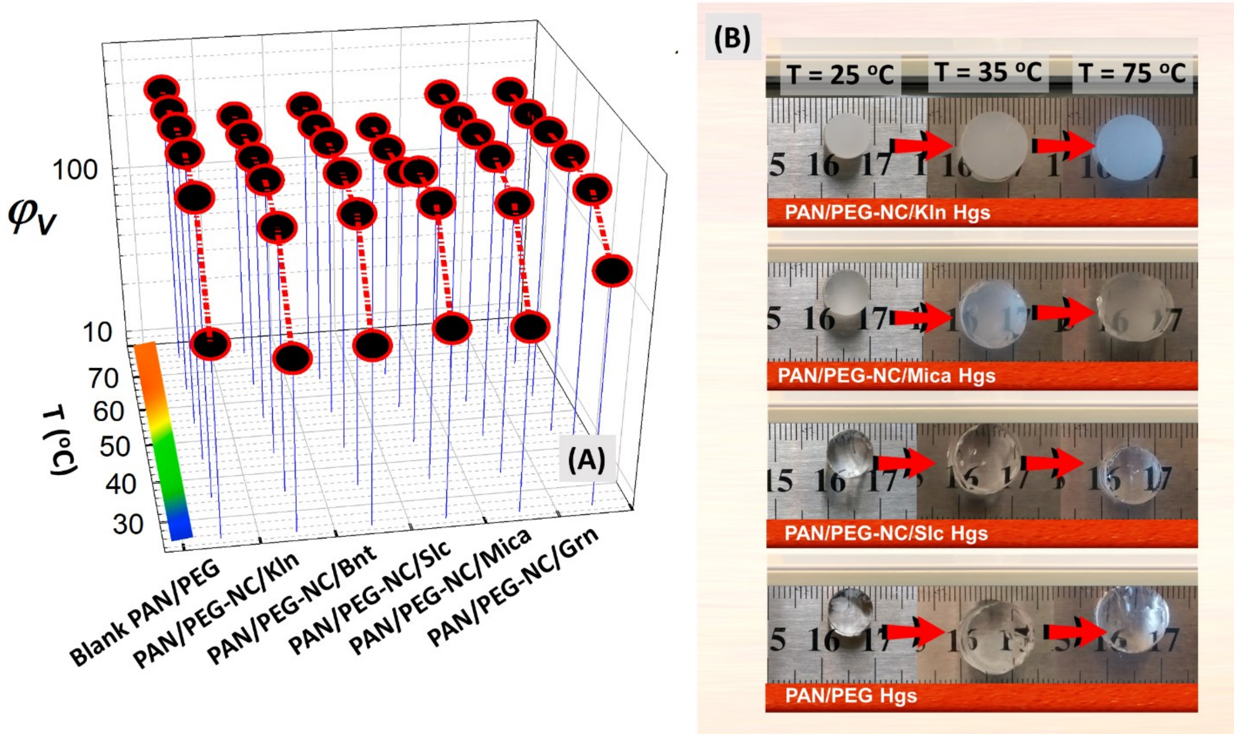


**Figure S6.** The equilibrium volume swelling ratio of hybrid hydrogels as a function of swelling temperature (A), and optical images for temperature-dependent swelling hybrid gels containing Kln, Mica and Slc (B).

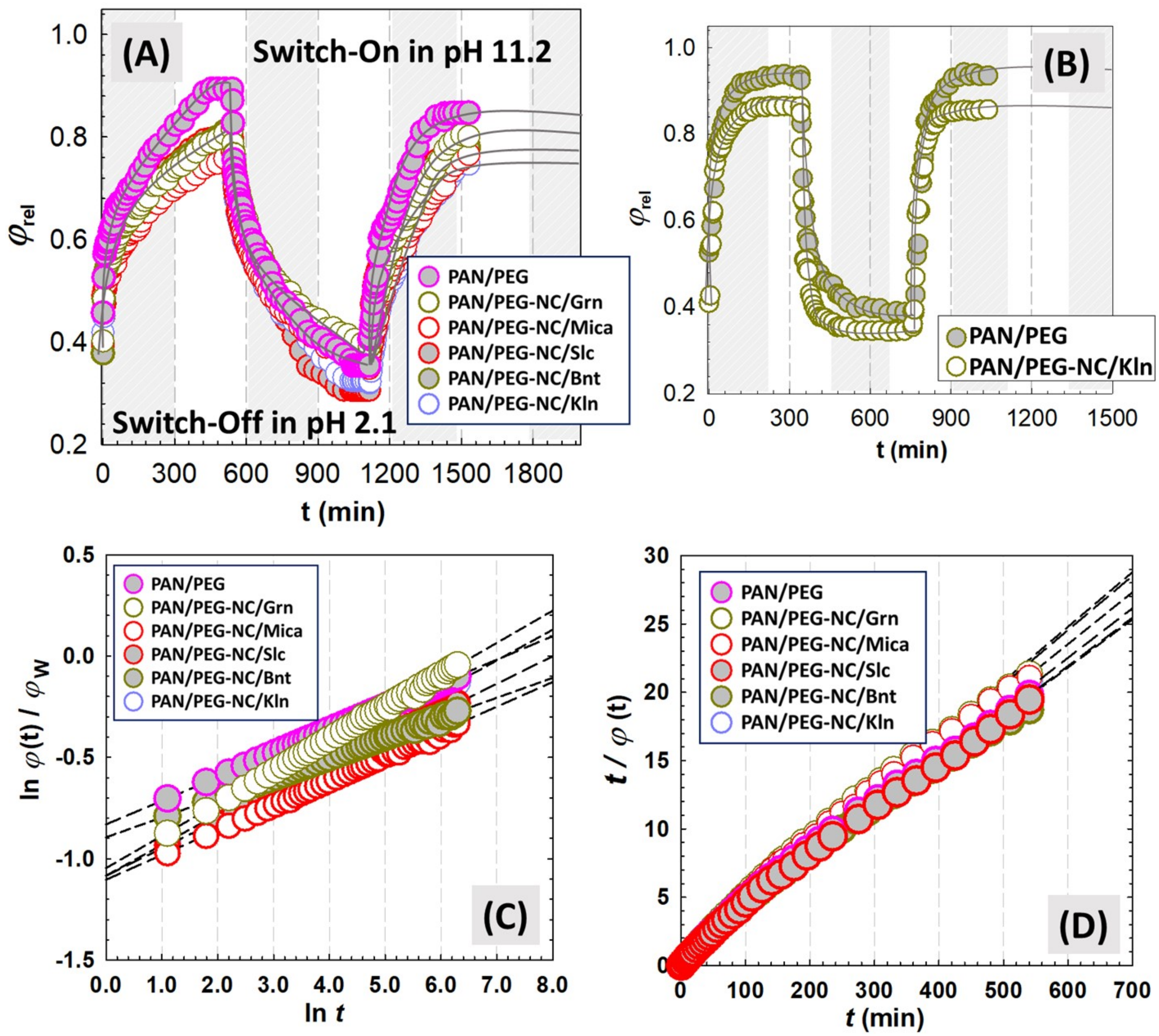


**Fig. S7.** (A, B) Reversible pulsatile swelling (pH 11.2) and deswelling (pH 2.1) of hybrid PAN/PEG-NC gels shown as the variation of relative gel mass $\varphi_{rel}$ with the time of swelling or shrinking, (C) $\ln \varphi(t)/\varphi_W$ against ln*t* plot, and (D) Schott kinetic model for average swelling rate $t/\varphi(t)$ obtained from the swelling in pH 11.2 solution.

**Table S5.** Non-linearized forms of the swelling kinetics equation applied in the swelling kinetics of ternary hybrid gels.

| | Type of Kinetic Model | Kinetic Equation | Description of coefficients |
|---|---|---|---|
| Eq. (S1) | Peppas power law equation model | $\frac{\varphi(t)}{\varphi_W} = kt^n$, $\varphi(t)/\varphi_W \leq 0.60$ | k is the swelling kinetic constant and n is the transport exponent. |
| Eq. (S2) | Schott's pseudo second order kinetics | $\frac{d\varphi(t)}{dt} = k_S\left[\varphi_W - \varphi(t)\right]^2$ $\frac{t}{\varphi(t)} = \frac{1}{k_s\varphi_W^2} + \frac{t}{\varphi_W}$ | $d\varphi(t)/dt$ is the time-dependent swelling velocity, and $k_s$ is the second order swelling rate constant. |

**Table S6.** Dynamic swelling characteristics; the kinetic exponent *n*, diffusion constant *k*, and swelling rate constant $k_s$ for hybrid PAN/PEG-NC gels from the swelling in pH 11.2 solution.

| | Fickian diffusion model | | | Schott's second-order kinetic model | |
|---|---|---|---|---|---|
| **Sample** | ***n*** | ***k*** | ***$R^2$*** | ***$k_S \times 10^{-1}$*** | ***$R^2$*** |
| **PAN/PEG** | 0.1026 | 0.4047 | 0.9610 | 0.1768 | 0.9761 |
| **PAN/PEG-NC/Kln** | 0.1310 | 0.3479 | 0.9831 | 0.2039 | 0.9985 |
| **PAN/PEG-NC/Bnt** | 0.1153 | 0.4355 | 0.9934 | 0.1711 | 0.9802 |
| **PAN/PEG-NC/Mica** | 0.1508 | 0.3085 | 0.9880 | 0.1976 | 0.9970 |
| **PAN/PEG-NC/Slc** | 0.1388 | 0.3341 | 0.9996 | 0.1890 | 0.9950 |
| **PAN/PEG-NC/Grn** | 0.1427 | 0.3106 | 0.9825 | 0.2113 | 0.9991 |

**Table S7.** The equations used for pseudo-first-order, pseudo-second-order, Elovich, Avrami kinetic, and intra-particle model for total MB adsorption onto various nanofiller-doped hybrid gels.

| | Adsorption Kinetic Model | Linearized Equation | Non-linearized Equation | Kinetic parameters |
|---|---|---|---|---|
| **Eq.(S3)** | Pseudo-First-order | $\ln(q_e - q_t) = \ln q_e - k_1 t$ | $q_t = q_e(1 - e^{-k_1 t})$ | $k_1$ is pseudo-first-order rate constant ($min^{-1}$) |
| **Eq.(S4)** | Pseudo-Second-order | $\frac{t}{q_t} = \frac{t}{q_e} + \frac{1}{k_2 q_e^2}$ | $q_t = \frac{k_2 q_e^2 t}{1 + k_2 q_e t}$ | $k_2$ is pseudo-second-order rate constant (g $mg^{-1}$ $min^{-1}$) |
| **Eq.(S5)** | Elovich | $q_t = \frac{1}{\beta}\ln t + \frac{1}{\beta}\ln(\alpha\beta)$ | $q_t = \frac{1}{\beta}\ln(\alpha\beta t)$ | α is a constant for rate of chemisorption, β is a constant for extent of surface coverage of adsorbent |
| **Eq.(S6)** | Avrami | $\ln\left[\ln\left(\frac{q_e}{q_e - q_t}\right)\right] = n_{Av}\ln k_{Av} + n_{Av}\,]$ | $q_t = q_e\left[1 - e^{\left[-(k_{Av}\ t)^{n_{Av}}\right]}\right]$ | $k_{Av}$ is Avrami kinetic constant, and $n_{Av}$ is Avrami exponent |
| **Eq.(S7)** | Intraparticle diffusion model | $q_t = k_{diff} t^{1/2} + C$ | $q_t = k_{diff} t^{1/2}$ | $k_{diff}$ is rate constant for intraparticle diffusion (mg $g^{-1}$ $min^{-1/2}$), and $C$ is a constant for thickness of boundary layer. |

**Table S8.** Thermodynamic parameters and energetic changes associated with adsorption of MB dye and adsorption capacity of nanofiller-doped hybrid PAN/PEC-NC/Clay gels.

| Sample | Exp. $q_e$ (mg/g) | Non-linear PFO $q_e$ (mg/g) | Non-linear PSO $q_e$ (mg/g) | $\Delta G^o$ (kJ/mol K) |
|---|---|---|---|---|
| **Blank PAN/PEG** | 6.0538 | 5.9381 | 6.3386 | -4.4862 |
| **PAN/PEG-NC/Kln** | 5.4050 | 5.1216 | 5.6564 | -2.9467 |
| **PAN/PEG-NC/Bnt** | 4.0615 | 3.9277 | 4.0853 | -0.7652 |
| **PAN/PEG-NC/Slc** | 6.1125 | 5.9518 | 6.3543 | -4.6233 |
| **PAN/PEG-NC/Mica** | 4.7692 | 4.6268 | 5.1356 | -1.8343 |
| **PAN/PEG-NC/Grn** | 6.9923 | 6.4833 | 7.1694 | -12.165 |

**Table S9.** The comparison of linearized PSO and intraparticle diffusion kinetic models' rate constants calculated from the experimental data.

| Pseudo-second order model (PSO) | | | Intra-particle model | | | |
|---|---|---|---|---|---|---|
| Sample | $k_2 \times 10^{-1}$ (g / mg min$^{-1}$) | $R^2$ | $k_{initial}$ (mg g$^{-1}$ min$^{-1/2}$) | $R^2$ | $k_{later} \times 10^{-}$ (mg g$^{-1}$ min$^{-1/2}$) | $R^2$ |
| **Blank PAN/PEG** | 0.21518 | 0.9993 | 0.6095 | 0.9936 | 0.1038 | 0.7021 |
| **PAN/PEG-NC/Kln** | 0.1109 | 0.9997 | 0.5621 | 0.9881 | 0.6271 | 0.9078 |
| **PAN/PEG-NC/Bnt** | 1.7821 | 0.9999 | 0.5506 | 0.9619 | 0.0888 | 0.7531 |
| **PAN/PEG-NC/Slc** | 0.2821 | 0.9995 | 0.6849 | 0.9866 | 0.1763 | 0.5714 |
| **PAN/PEG-NC/Mica** | 0.1219 | 0.9993 | 0.5582 | 0.9992 | 0.5985 | 0.7614 |
| **PAN/PEG-NC/Grn** | 0.0829 | 0.9994 | 0.7562 | 0.9691 | 1.0956 | 0.7529 |

**Table S10.** Non-linearized forms of the isotherm models applied in the adsorption of MB dye.

| | Types of Isotherm Model | Non-linear Equation | Isotherm parameters | Description of Isotherm |
|---|---|---|---|---|
| **Eq.(S8)** | Langmuir | $q_e = \frac{q_{\max} K_L C_e}{1 + K_L C_e}$ | $q_{\max}$ (mg g$^{-1}$) is maximum adsorption capacity of adsorbent, $K_L$ (L/mg) is Langmuir adsorption constant, $R_L$ is separation factor | $R_L$ value shows that adsorption process is irreversible for $R_L = 0$, is favorable for $0 < R_L < 1$, linear for $R_L = 1$ or unfavorable for $R_L > 1$ |
| **Eq.(S9)** | Freundlich | $q_e = K_F C_e^{1/n_F}$ | $K_F$ (mg/g)(mg/L)$^{-1/n}$ is Freundlich isotherm constant and $n_F$ is adsorption intensity | $n_F$ is heterogeneity factor and $1/n_F < 1$ confirms a cooperative adsorption. |
| **Eq.(S10)** | Redlich-Peterson (R-P) isotherm | $q_e = \frac{K_{RP} C_e}{(1 + \alpha_{RP} C_e^{\beta_{RP}})}$ | $K_{RP}$ (L/g) is Redlich−Peterson isotherm constant, $\alpha_{RP}$ (mg/L) is Redlich–Peterson model constant and $\beta_{RP}$ are Redlich-Peterson model exponent | $\beta_{RP}$ is Redlich–Peterson model exponent, should be $0 \le \beta \le 1$. |
| **Eq.(S11)** | Sips isotherm | $q_e = \frac{q_{\max} K_S C_e^{n_S}}{(1 + K_S C_e^{n_S})}$ | $K_S$ is Sips equilibrium constant (L mg$^{-1}$), $n_S$ is Sips model exponent. | If value of $n_S$ is equal to 1 then this equation will become a Langmuir equation. As $C_e$ or $K_S$ approaches 0, this isotherm reduces to Freundlich isotherm. |
| **Eq.(S12)** | Dubinin-Radushkevich (D-R) | $q_{\max} = q_e e^{-K_{DR}\varepsilon^2}$ | $\varepsilon$ (J/mol) is potential of Polanyi, E is the mean adsorption energy and $\beta$ is D-R isotherm constant | D–R model provides information on the sorption process, whether it be |

| | | |
|---|---|---|
| | ($mol^2$ / $J^2$) | chemisorption or physisorption. |

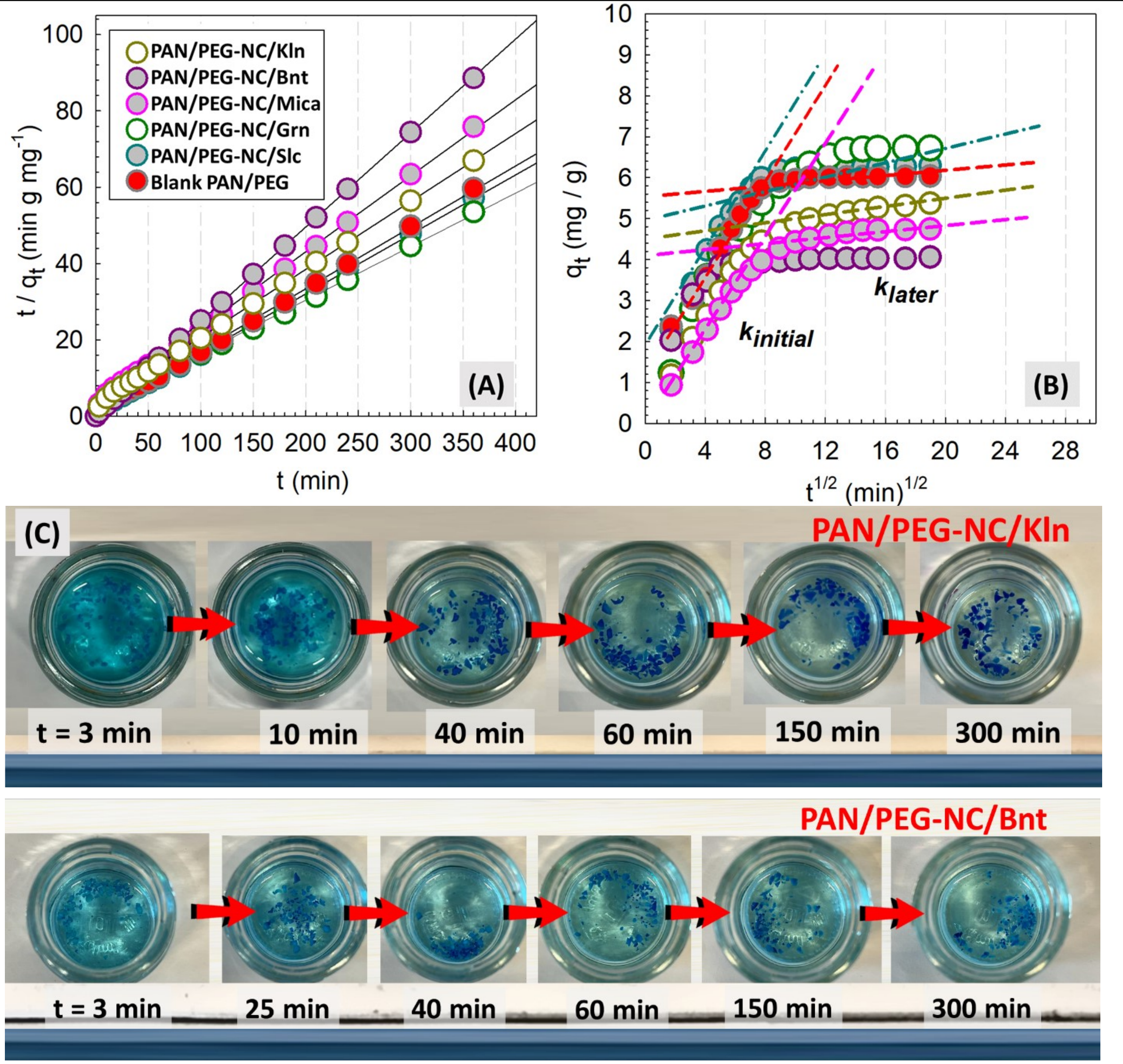


**Figure S8.** Regression analysis of adsorption of MB with PAN/PEG and hybrid PAN/PEC-NC gels containing Kln, Bnt, Mica, Grn, and Slc by pseudo-second order (PSO) kinetic model (A), and intra-particle diffusion model (B) and optical views of Kln and Bnt-integrated PAN/PEG-NC gels during adsorption (C).

**Table S11.** Comparison of the results obtained from this study with other adsorbents used in MB adsorption.

| Adsorbents | Dye Name | Kinetic Model | Isotherm Model | Adsorbent Dose | Dye Concentration | $q_{max}$ (mg/g) | Ref. |
|---|---|---|---|---|---|---|---|
| Kaolin-integrated sodium alginate graft poly(acrylic acid-co-acrylamide) | Rhodamine B | Pseudo second-order | Freundlich and Redlich-Peterson equations | 0.05-0.5 g | 1000mg/L, pH=7, contact time 24 h, temperature 20 °C | 245 mg/g | [8] |
| Carboxymethyl cellulose grafted by polyacrylic acid and decorated with graphene oxide | Methylene blue | Pseudo second-order | Langmuir | (0.01, 0.025, 0.05, 0.075, and 0.1 g) | 50 mL solution (100 mg/mL) constant stirring at 100 rpm | 48–94% and capacity 58–110 mg/g | [9] |
| Polyvinyl alcohol/carboxymethyl cellulose hydrogels reinforced with graphene oxide and bentonite | Methylene blue | Pseudo second-order | Langmuir | 30 mg | 20 mL of aqueous solution of 200 mg/L at room temperature | 172.14 mg/g | [10] |
| Carrageenan-g-polyacrylamide/bentonite superabsorbent composites | Methylene blue | Not-specified | Langmuir | 20 mg | 50 mL of 20-90 mg / L | 43.6-123.75 mg g−1 | [69] |
| Glucose and glucosamine grafted polyacrylamide/graphite composites | Methylene blue | Pseudo second-order | Langmuir | 0.02 g to 0.120 g | 50 mL of 10 to 100 mg/L | 61% to 90.33% | [80] |
| PAN/PEG-NC gels doped with BNT, Kln, Mica, Slc, and Grn | Methylene blue | Pseudo second-order | Sips and Langmuir | 0.01 g | 20 mL of 20 to 100 mg/L | 57.6%, 67.7%, 76.6%, 88.6% 99.2% (84.8 - 95.1 mg/g) | This work |